DOI: 10.1007/s11099-016-0674-z PHOTOSYNTHETICA 55 (4): 588-602, 2017

Inhibition of root respiration induces leaf senescence in *Alhagi sparsifolia*

G.-L. TANG[*,**], X.-Y. LI[*,**,+], L.-S. LIN[*,**], Y HU[***], and F.-J. ZENG[*,**]

State Key Laboratory of Desert and Oasis Ecology, Xinjiang Institute of Ecology and Geography, Chinese Academy of Sciences, Urumqi 830011, China[*]
Cele National Station of Observation and Research for Desert-Grassland Ecosystem in Xinjiang, Cele 848300, Xinjiang, China[**]
College of Grassland and Environmental Sciences, Xinjiang Agricultural University, Urumqi 830052, China[***]

Abstract

Leaf senescence can be induced by numerous factors. In order to explore the relationship between root respiration and leaf senescence, we utilized different types of phloem girdling to control the root respiration of *Alhagi sparsifolia* and its physiological response. Our results showed that both girdling and inhibition of root respiration led to a decline of stomatal conductance, photosynthesis, transpiration rate, chlorophyll (Chl) *a*, Chl *b*, carotenoid (Car) content, Chl *a*/*b*, Chl/Car, water potential, and Chl *a* fluorescence, as well as to an increase of abscisic acid (ABA), proline, and malondialdehyde content in leaves and to upregulation of senescence-associated gene expression. Our present work implied that both inhibition of root respiration and girdling can induce leaf senescence. In comparison with phloem girdling, the leaf senescence caused by inhibition of root respiration was less significant. The reason for girdling-induced senescence was ABA and carbohydrate accumulation. Senescence induced by inhibition of root respiration occurred due to leaf water stress resulting from inhibition of water absorption.

Additional key words: carbohydrate; chlorophyll; girdling; phloem transport; photosynthetic pigment.

Introduction

Constituting the last stage of leaf development in plants (Fukao *et al.* 2012, Sakuraba *et al.* 2012), leaf senescence is an active phase of plant development involving well-orchestrated degradation and remobilization processes (Yordanov *et al.* 2008, Besseau *et al.* 2012, Gregersen *et al.* 2013, Kotakis *et al.* 2014). Leaf senescence starts from chloroplast decomposition, followed by catabolism of macromolecules, such as Chl, protein, lipids, and RNA (Hopkins *et al.* 2007, Lim *et al.* 2007, Besseau *et al.* 2012), while the nucleus and mitochondria remain active for a long period of time during senescence (Lim *et al.* 2007, Roberts *et al.* 2012). Leaf senescence is induced by numerous factors, such as darkness (Buchanan-Wollaston *et al.* 2005, Gregersen *et al.* 2013), high light intensity (Fu

Received 3 June 2016, *accepted* 7 September 2016, *published as online-first* 15 November 2017.
[+]Corresponding author; phone: +86 991 7885320, e-mail: lixy@ms.xjb.ac.cn
Abbreviations: ABA – abscisic acid; ABS/RC – absorption flux (of antenna Chls) per RC (also a measure of PSII apparent antenna size); Car – carotenoids; Chl – chlorophyll; CS – cross section of the sample; DI_o/RC – dissipation flux per RC; DM – dry mass; *E* – transpiration rate; ET_o/RC – electron transport flux (further than Q_A^-) per RC; F_v/F_m – maximum photochemical efficiency of PSII; FM – fresh mass; G1 – girdling with one branch left; G2 – girdling with two branches left; g_s – stomatal conductance; JA – jasmonic acid; MDA – malondialdehyde; M_o – approximated initial slope of the fluorescence transient; N1 – nongirdling with one branch left; N2 – nongirdling with two branches left; OEC – oxygen-evolving complex, PI_{abs} – performance index on absorption basis; P_N – net photosynthetic rate; PQ – plastoquinone; Pro – proline; RC – reaction center; RC/CS – density of RCs (Q_A^-reducing PSII reaction centers); SA – salicylic acid; SAGs – senescence-associated genes; S_m – normalised total complementary area above the OJIP transient (reflecting single-turnover Q_A reduction events); TBA – thiobarbituric acid; TR_o/RC – trapped energy flux (leading to QA reduction) per RC; ψ_o – probability that a trapped exciton moves an electron into the electron transport chain beyond Q_A^- (at t = 0); φ_{Eo} – quantum yield for electron transport (at t = 0); φ_{Po} – maximum quantum yield for primary photochemistry; Ψ_{leaf} – leaf water potential; Ψ_M – midday water potential; Ψ_P – predawn water potential.
Acknowledgments: We thank the anonymous reviewers for valuable comments. We also express gratitude to Zhuyu Gu for assistance with experiment, and Jake Carpenter for polishing the English in this manuscript. This research was supported by National Natural Sciences Foundation of China (41571057), Key Program of Joint Funds of the National Natural Sciences Foundation and the Government of Xinjiang Uygur Autonomous Region of China (U1203201), and the National Natural Sciences Foundation of China (41371516).

et al. 2012), high light dosage (Noodén *et al.* 1997, Gregersen *et al.* 2013), heat (Lobell *et al.* 2012, Gregersen *et al.* 2013), water stress (Yang *et al.* 2003), nitrogen starvation (Koeslin-Findeklee *et al.* 2014), salicylic acid (SA) (Vogelmann *et al.* 2012), ABA (Setter *et al.* 1980, Gregersen *et al.* 2013), jasmonic acid (JA) (Jiang *et al.* 2014), cytokinins (Zwack *et al.* 2013), gibberellin (GA) (Chen *et al.* 2014), carbon starvation (Brouquisse *et al.* 2001, Parrott *et al.* 2005), carbon feast (Moore *et al.* 2003, Parrott *et al.* 2005), disease (Robert-Seilaniantz *et al.* 2011, Gregersen *et al.* 2013) *etc*. Traditionally, accepted ideas regarding senescence mechanisms fall into two main categories: nutrient deficiency and genetic programming (Noodén *et al.* 1997). However, an increasing amount of evidence indicates that genetic programming, rather than nutrient deficiency, is the central senescence program component (Noodén *et al.* 1997, Parrott *et al.* 2005, 2007, Gregersen *et al.* 2013).

Many studies have demonstrated that phloem girdling can induce leaf senescence (Dai and Dong 2011, Parrott *et al.* 2005, 2007); however, the underlying mechanisms of girdling-caused leaf senescence are poorly understood (Dai and Dong 2011). In the girdling system, a removal of a ring of phloem disrupts the basipetal movement of photosynthetic products through the phloem, which results in the accumulation of carbohydrates in leaves (Rivas *et al.* 2006, Urban and Alphonsout 2007, Yang *et al.* 2013), and thus leads to carbon feast-induced leaf senescence (Parrott *et al.* 2005). This process may be associated with many different genes (Parrott *et al.* 2007, 2010). In addition, girdling also results in the decrease of cytokinins (Dai and Dong 2011) and increase of ABA (Setter *et al.* 1980, Dai and Dong 2011) in the leaf, which may constitute another mechanism of induced leaf senescence (Dai and Dong 2011). However, only scant literature associated leaf senescence with a root status, in spite of numerous studies showing that girdling can lead to a decrease in dry root mass (Dai and Dong 2011), low root starch content (Frey *et al.* 2006), and low root respiration (Högberg *et al.* 2001, Bhupinderpal-Singh *et al.* 2003, Subke *et al.* 2004, Frey *et al.* 2006). Since girdling leads to a decline of root respiration (Högberg *et al.* 2001, Johnsen *et al.* 2007) and to an increase in the expression of certain genes involved in carbohydrate metabolism (Li *et al.* 2003, Parrott *et al.* 2005, 2007, Pourtau *et al.* 2006), it makes easy testing the relationship between foliar parts and root systems in many plant species (Dai and Dong 2011).

Previous studies have shown that removal of roots causes a decrease in protein content and enhances senescence in leaves (Sitton *et al.* 1967). The mechanism seems to involve changes in cytokinin contents, formed in roots and translocated with the transpiration stream through the xylem to shoots, which affect the leaf senescence process (Sitton *et al.* 1967). The cytokinins and ABA in roots may be a key factor influencing leaf senescence (Yang *et al.* 2002). Tschaplinski and Blake (1985) described that imbalanced root/shoot ratios caused internal water stress, resulting in the inhibition of stomatal opening, and also resulted in leaf and whole plant senescence. Recent studies demonstrated that Fe-deficiency in roots induced expression of many senescence-associated genes related to lipid peroxidation, which are linked to typical senescence pathways (Sperotto *et al.* 2008). In addition, plant senescence may also be regulated by root depth (Kong *et al.* 2013).

A relationship between root status and leaf senescence has been already found; however, it has not been well studied how leaf senescence is linked to root respiration. In the girdling system, leaf senescence has been attributed to a root status, even though the phloem girdling has always exhibited a negative effect on roots. Thus, in this study, we performed two different types of girdling in order to control root respiration and maintain the aboveground part of *A. sparsifolia* in the same conditions. Some senescence-associated physiological indicators were investigated to evaluate the extent of leaf senescence. The objective of this paper was to elucidate whether and how leaf senescence is influenced by root respiration and identify physiological characteristics during different types of senescence in *A. sparsifolia*.

Materials and methods

Plant material: *Alhagi sparsifolia* Shap. was used for this study. This plant is a spiny, clonal, perennial leguminous herb growing in arid and semiarid regions with few leaves, and is about 1 m tall. It is widely distributed in a transition zone between the oasis and desert in the southern fringe of the Takalimakan Desert in Western China, and is one of the important dominant species in this region. We chose *A. sparsifolia* as our plant material because it is a deep-rooted plant. *A. sparsifolia* has a large root/shoot ratio and the roots accounted for a large part of the whole plant. So, compared with other plants, the effect of the root status on the aboveground portion of *A. sparsifolia* plant might be greater than in other plant species.

Study region: The experiment was performed at the Desert Experimental Area in Cele National Field Research Station for Desert Steppe Ecosystems, Chinese Academy of Sciences. The research area is located in the Taklimakan Desert at the oasis-desert transitional zone on the southern rim of the Taklimakan Desert (35°17′55″–39°30′00″N, 80°03′24″–82°10′34″E).

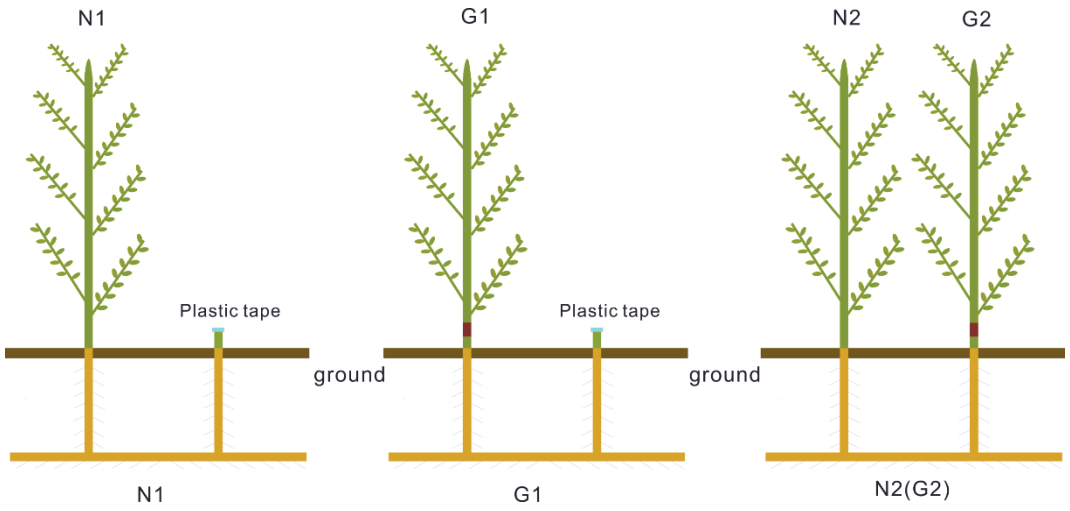

Fig. 1. Illustration of treatment of *Alhagi sparsifolia* phloem girdling. N1 – nongirdling with one branch left; G1 – girdling with one branch left; N2 – nongirdling with two branches left; G2 – girdling with two branches left. The green parts are leaves or stems, the yellow parts are roots, and the red parts represent the girdle. The girdle is about 10 mm wide, covered with silicon grease, and wrapped in adhesive plastic tape to prevent desiccation. The blue parts represent the plastic tape, which was placed on the cut after being covered with silicon grease. The brown parts represent the soil and ground. We also cut other branches, which are not shown in the illustration. The growth directions of the leaves are random, and are also not shown in the illustration.

Experimental design: In early September 2013, a 30 m × 30 m quadrat was selected in the oasis-desert transitional zone. Thirty plants of *A. sparsifolia* with a similar size and growth were selected for treatments within the quadrat. Two different types of girdling were performed. For the first treatment, we chose 20 plants and pruned off redundant branches, with only one branch remaining. From those 20 plants, we selected 10 plants (group 1) for girdling (denoted as G1, girdling with one branch left), and the other plants (group 2) were not treated with girdling (N1, nongirdling with one branch left). For the second treatment, we chose 10 plants of *A. sparsifolias* and pruned off redundant branches with two branches remaining. For this treatment, one of two remaining branches was treated with girdling (group 3, denoted as G2, girdling with two branches left), while in the group 4, both branches were not treated with girdling (denoted as N2, nongirdling with two branches left). Thus, in the first treatment, G1 and N1, each plant consisted of one branch connected to roots; in the second treatment, G2 and N2, each plant consisted of two branches connected to roots (Fig. 1).

When the branches were pruned, cut regions were immediately covered with silicon grease and wrapped in adhesive plastic tape to prevent desiccation. The same treatment was performed at the girdled regions. After pruning of redundant branches, various parameters were measured. Our data showed that there were no statistical differences between treatments (N1, G1, N2, and G2) (Fig. 1; Table 1S, *supplement available online*). Then, we began to girdle the branches. After 30 d of girdling, we started our measurements of soluble sugar content, starch content, root respiration, ABA content, net photosynthetic rate (P_N), stomatal conductance (g_s), transpiration rate (E), photosynthetic pigment content, leaf water potential (Ψ_{leaf}), proline (Pro) content, malondialdehyde (MDA) content, and chlorophyll (Chl) fluorescence. Either before or after girdling, we took a portion of roots for measurement of root soluble sugar content, root starch sugar content, and root respiration. For the aboveground parts of the plants, the treatment of N1 was the same as N2, and G1 was the same as G2; thus, if there was any statistical difference between N1 and N2 or G1 and G2, it should be attributed to the influence of the underground parts of the plants, *i.e.* roots.

g*$_s$, *P*$_N$, and *E were measured in the field using the portable photosynthesis system (*LI-COR 6400*, *LI-COR Inc.*, Lincoln, NE, USA) according to Mittler *et al.* (2001). The parameters were measured prior and 30 d after girdling. All measurement days were cloudless. We conducted measurements at 10:00 h (GMT+6), when the P_N of plants was the greatest during the day. The photosynthetically active radiation (PAR) was about 1900 μmol m^{-2} s^{-1}, concentration of the CO_2 was about 380 μmol mol^{-1}, and relative humidity (RH) was about 30%.

As the measured leaves did not reach the standard size of a leaf chamber (2 cm × 3 cm), a scanner and *Image Pro Plus 6.0* software (*Media Cybernetics*, Silver Springs, MD, USA) were used to determine the surface area of the measured leaves, and it was later utilized to calculate the actual values of P_N, g_s, and E. Ten replicate measurements were performed for each treatment. We selected the third leaf (count from top to base) on the branch for the measurement.

Photosynthetic pigment content, ABA, soluble sugar, and starch: All leaves were of a similar size and selected from the second to fifth leaves on each of the branches. We picked five leaves from each *A. sparsifolia*, thus each treatment (N1, G1, N2, and G2) included 50 leaves (5 × 10). Determination of photosynthetic pigment contents was described by Lichtenthaler (1987). Specifically, for every 10 leaves (we divided 50 leaves into 5 groups, each group contained 10 leaves), Chl was extracted with mortar and pestle in 10 mL of 80% chilled acetone with 5 g of $MgCO_3$ and purified sea sand. After centrifugation at 2,500 rpm for 2 min, Chl *a*, Chl *b*, and carotenoids (Car) were determined spectrophotometrically at 663, 647, and 470 nm, respectively (*Jenway 6400*, *Krackeler Scientific*, London, UK). The concentration was calculated as previously described by Lichtenthaler (1987). Five replicates were performed for each treatment.

We picked 10 leaves and 10 roots from each *A. sparsifolia* plant, and thus each treatment comprised of 100 leaves (10 × 10) and 100 roots (10 × 10). The leaves and roots were dried at 75°C for 24 h until the mass was maintained stable. Then, the dried leaves were ground to powder. The leaf powder (0.5 g) and root powder (0.5 g) were, respectively, extracted with 4 mL of 80% ethanol at 80°C for 40 min, followed by two extractions with 2 mL of 80% ethanol. The supernatants were combined and purified by 10 g of activated carbon at 80°C for 30 min. Ethanol (80%) was added to the extracts in order to maintain a constant volume (10 mL) for measuring the amount of soluble sugar (Li *et al.* 2011). The remaining sample (after measurement of soluble sugar) was dried at 45°C to remove ethanol, and boiled for 10 min with 3 mL of double-distilled water in 7.5-mL centrifuge tubes. The samples were then cooled to room temperature (28°C), and 4 mL of $HClO_4$ was added to decompose the starch and hydrolyzed for 15 min. Soluble sugar (mainly glucose) was measured at 630 nm (*Jenway 6400*, *Krackeler Scientific*, London, UK) as described previously by Li *et al.* (2011). Starch content was calculated using the formula (Tang *et al.* 2015a):

Starch content [%] = G (glucose mass obtained from a standard curve) × 0.9 (coefficient of glucose converted to starch)/dry mass (DM) × 100%

ABA extraction was determined by the method described by Veselov *et al.* (2008). All samples were taken in the morning at about 10:00 h, weighed, and then frozen in liquid nitrogen. Frozen samples were ground to fine powder in liquid nitrogen. ABA was extracted in 80% ethanol and incubated overnight at 4°C. Distilled water was added to dilute the aqueous residue, then acidified with HCl (1 mol L^{-1}) to pH 2.5, then partitioned twice with peroxide-free diethyl ether (ratio of organic to aqueous phases was 1:3). The organic phase was transferred into 1% sodium hydrocarbonate (pH 7–8, ratio of organic to aqueous phases was 3:1). The solution was re-extracted with diethyl ether, methylated with diazomethane, and immunoassayed using antibodies to ABA (Vysotskaya *et al.* 2004). More details about the method and calculations can be found in Veselov *et al.* (2008).

Pro, MDA content, and root respiration: The measurement of Pro content was performed according to the method described by Demiral and Türkan (2005). Fresh leaves of 0.5 g were ground and mixed with 5 ml of 3% (w/v) sulfosalicylic acid. The samples were then filtered through filter paper. After addition of acid ninhydrin and glacial acetic acid, resulting mixture was heated at 100°C for 1 h in a water bath. The mixture was then placed in an ice bath for about 30 min. The mixture was extracted with 25 ml of toluene, which was taken as a control. The extract was then placed in a cuvette, and its absorbance was measured at 520 nm (*Jenway 6400*, *Krackeler Scientific*, London, UK). The Pro content was calculated using a calibration curve and expressed as mol(Pro) g^{-1}(fresh mass, FM).

The determination of MDA content was based on the method described by Rahman *et al.* (2012). Thiobarbituric acid (TBA) reactive substances representing lipid-peroxidation products were extracted after homogenization of a 0.2 g leaf sample in 5 mL of solution containing 20% trichloroacetic acid and 0.5% 2-TBA. The mixture was heated at 95°C for 30 min, and the reaction was stopped in an ice bath. The cooled mixture was centrifuged at 5,000 × *g* for 10 min at 25°C, and the absorbance of the supernatant at 532 and 600 nm were recorded (*Jenway 6400*, *Krackeler Scientific*, London, UK). After subtracting the nonspecific turbidity at 600 nm, the MDA content was determined by its molar extinction coefficient, 155 M cm^{-1} per FM (Rahman *et al.* 2012).

Fresh fine roots (diameter < 2 mm) were taken from each plant and properly mixed. The sample was used to measure a root respiration rate utilizing the liquid-phase oxygen measurement system (*Hansatech Ltd.,* King's Lynn, Northfolk, UK) at a temperature of 25°C. Five replicate measurements were performed for each treatment, more details described by Liu *et al*. (2013).

Ψ_{leaf} readings were performed according to previous studies (Williams and Araujo 2002, Williams *et al.* 2012). Predawn water potential (Ψ_P) measurements began at about 4:30 h (GMT+6) and were finished before sunrise using a pressure chamber (*PMS Instruments Co.*, Corvallis, Oregon, USA). Midday water potential (Ψ_M) measurements were performed between 11:30 and 12:30 h. (GMT+6). Leaf blades used for the determination of Ψ_{leaf} were covered with a plastic bag, and quickly sealed. Petioles were then cut within 1 to 2 s, and the time between leaf excision and chamber pressurization was generally < 10 to 15 s. Leaves chosen for Ψ_M determinations were exposed to direct solar radiation, PPFD was about 2,100 μmol m^2 s^{-1}.

Chl fluorescence measurement was carried out according to the procedures of Tang *et al.* (2015b). Chl *a* fluorescence was induced by a saturated PPFD at 3,500 mmol m^{-2} s^{-1} provided by an array of three light-emitting diodes (peak 650 nm) to generate fluorescence curves expanding from F_o to F_m for the four treatments (N1, N2, G1, and G2). Data were initially sampled at 10-μm intervals for the first 300 μm to achieve an excellent time resolution of dark-adapted F_o, as well as the initial rise kinetics. The time resolution of digitization was then switched to slower acquisition rates. The PSII parameters and OJIP transients were analyzed according to Strasser *et al.* (2000, 2004). Formulae and terms used in the analysis of the OJIP fluorescence induction dynamics curve are as follows:

Parameter	Description
F_o	Minimal recorded fluorescence intensity
F_m	Maximal recorded fluorescence intensity
t_{Fm}	Time to reach maximal fluorescence intensity F_m
$V_J = (F_J - F_o)/(F_m - F_o)$	Relative variable fluorescence intensity at the J-step
$M_o = 4\ (F_{300\mu s} - F_o)/(F_m - F_o)$	Approximated initial slope of the fluorescence transient
$S_m = (\text{Area})/(F_m - F_o)$	Normalised total complementary area above the OJIP transient (reflecting single-turnover Q_A reduction events)
$\text{ABS/RC} = M_o\ (1/V_J)(1/\varphi_{Po})$	Absorption flux per RC
$\text{TR}_o/\text{RC} = M_o\ (1/V_J)$	Trapped energy flux per RC (at t = 0)
$\text{ET}_o/\text{RC} = M_o\ (1/\text{VJ})\ \psi_o$	Electron transport flux per RC (at t = 0)
$\text{DI}_o/\text{RC} = (\text{ABS/RC}) - (\text{TR}_o/\text{RC})$	Dissipated energy flux per RC (at t = 0)
$\varphi_{Po} = \text{TR}_o/\text{ABS} = [1 - (F_o/F_m)]$	Maximum quantum yield for primary photochemistry (at t = 0)
$\Psi_o = \text{ET}_o/\text{TR}_o = (1 - V_J)$	Probability that a trapped exciton moves an electron into the electron transport chain beyond Q_A^- (at t = 0)
$\varphi E_o = \text{ET}_o/\text{ABS} = [1 - (F_o/F_m)]\ \psi_o$	Quantum yield for electron transport (at t = 0)
$\text{PI}_{abs} = (\text{RC/ABS})\ [\varphi_{Po}/(1 - \varphi_{Po})]\ [\psi o/(1 - \psi_o)]$	Performance index on absorption basis

Data analysis: The treatment effects (N1, G1, N2, and G2) were analyzed by one-way analysis of variance (*ANOVA*) using *PASW Statistics 18.0* software (*Macintosh*, *SPSS Inc*., Chicago, IL, USA) for each parameter (soluble sugar, starch, photosynthetic pigment content, ABA content, P_N, g_s, E, root respiration rate, Ψ_{leaf}, Chl fluorescence, Pro, and MDA content). LSD multiple range tests at $p<0.05$ were used to identify statistically significant differences. The results shown in the graphs are presented as the mean value ± SD.

Results

Soluble sugar, starch, root respiration characteristics and gene expression: As expected, girdling appeared to alter the transport of photoassimilates below ground, as soluble sugars and starch increased in leaves but declined in roots of the girded plants. However, the presence of the intact branch on the root system appeared to ameliorate the decline in root soluble sugars and starch, as these values declined less in the G2 compared to G1 treatment. Furthermore, the rates of root respiration corresponded with root carbohydrate and starch concentrations irrespective of treatments (Fig. 2).

ABA, g_s, P_N, and E: ABA increased significantly in the girdled leaves (G1, G2), which was similar to the change in photoassimilates. The g_s, P_N, and E declined significantly in the girdled leaves (Fig. 3).

ABA content in N1 and N2 leaf showed no significant difference, however, the difference in g_s, P_N, and E were significant between the N1 and N2 treatments. Compared with N1, g_s, P_N, and E in the N2 treatment decreased by 8.4, 12.6, and 10.8%, respectively (Fig. 3). This corresponded to the fact that root respiration rate declined in the N2 treatment compared with N1. The decline of P_N, as one of indicators of senescence, might indicate proceeding leaf senescence after the N2 treatment.

Photosynthetic pigments: The Chl content is another indicator of leaf senescence. Similar to P_N, girdling also significantly reduced Chl *a*, Chl *b*, Chl (*a*+*b*), Car, Chl *a*/*b*, and Chl/Car in the treated plants (Fig. 4). It indicated that girdling led to leaf senescence in *A. sparsifolia*. Inhibition

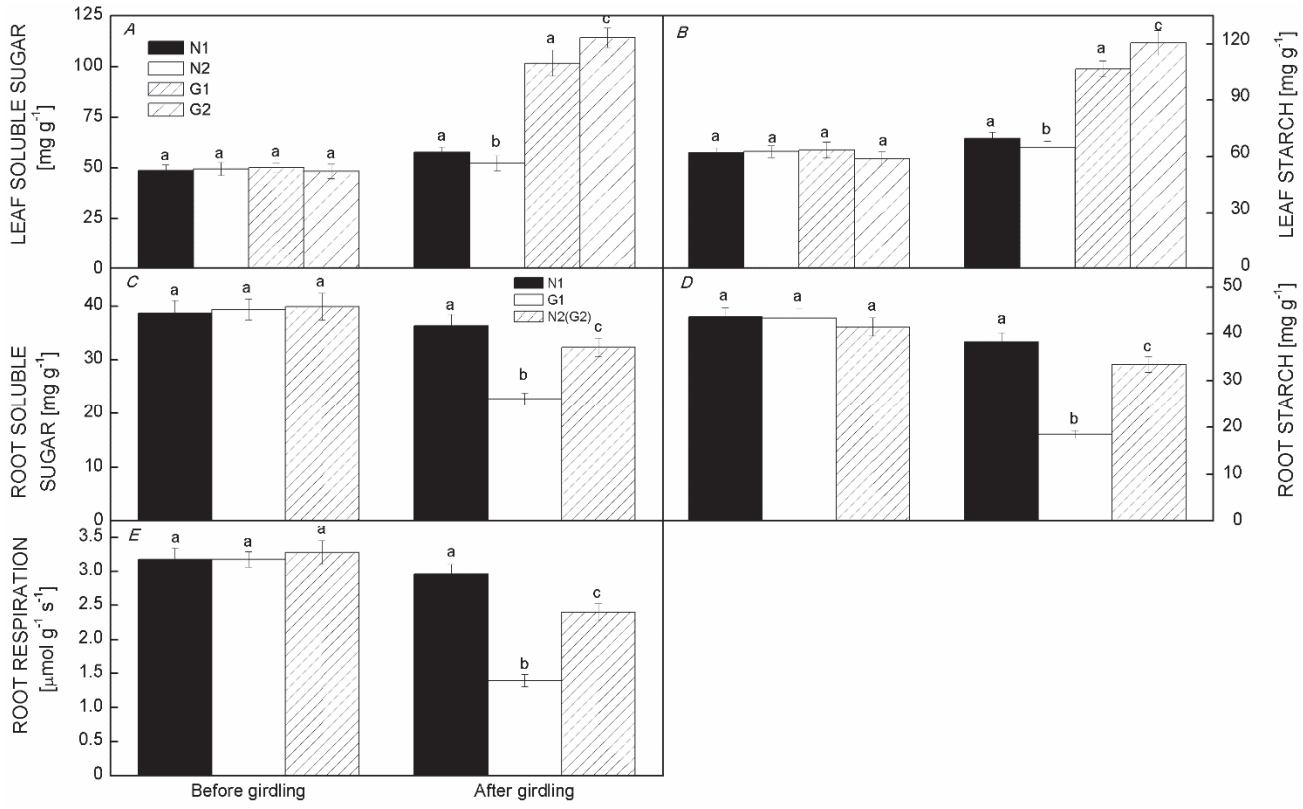

Fig. 2. Soluble sugar, starch, and root respiration of *Alhagi sparsifolia* under N1, N2, G1, and G2 treatment. *A*: leaf soluble sugar content, *B*: leaf starch content, *C*: root soluble sugar content, *D*: root starch content, *E*: root respiration of *Alhagi sparsifolia* before and after girdling. *Different letters* indicate significant difference (p<0.05). The data represent means of five biological replicates ± SD. N1 – nongirdling with one branch left; G1 – girdling with one branch left; N2 – nongirdling with two branches left; G2 – girdling with two branches left.

of root respiration also significantly lowered Chl *a*, Chl *b*, and Chl (*a*+*b*) by 10.8, 5.4, and 6.9%, respectively, in the N2 treatment compared with the N1 treatment. Although Car, Chl *a*/*b*, and Chl/Car also decreased in the N2 leaves compared with N1, the decline was mild and insignificant. In addition, the presence of the intact branch on the root system appeared to ameliorate the decline in Chl and Car contents, as they decreased less in the G2 relative to the G1 treatment (Fig. 4).

Water potential, Pro, and MDA: As expected, girdling appeared to lower Ψ_P and Ψ_M (Fig. 5), and increase significantly Pro and MDA contents (Fig. 6). Moreover, Ψ_P and Ψ_M declined significantly in the girdled leaves (G1, G2) compared with nongirdled leaves (N1, N2). Similar to the results above, the presence of the intact branch on the root system also appeared to ameliorate the change in Ψ_P, Ψ_M, Pro, and MDA, as these values changed less in the G2 relative to the G1 treatment (Figs. 5, 6). In addition, compared with N1, the value of Ψ_P and Ψ_M in the N2 treatment (Fig. 5) decreased by 15.4 and 8.7%, respectively, and Pro and MDA contents (Fig. 6) increased by 8.5 and 5.8%, respectively. The difference of Ψ_P, Ψ_M, Pro, and MDA in the N1 and N2 treatments may also result from inhibition of root respiration.

Chl *a* fluorescence characteristics: All parameters of Chl fluorescence showed insignificant differences before girdling (Fig. 7, Table 1S). After girdling (30 d), however, the measurements of the approximated initial slope of the fluorescence transient (M_o), absorption flux per reaction center (ABS/RC), and dissipated energy flux per reaction center (DI_o/RC) were lowered in the order of G1 > G2 > N2 > N1 (Fig. 6, Table 1S). On the contrary, the value in the normalised total complementary area above the OJIP transient (reflecting single-turnover of primary bound plastoquinone [Q_A] reduction events) (S_m), quantum yield for electron transport (at t = 0) (φ_{Eo}), probability that a trapped exciton moves an electron into the electron transport chain beyond Q_A^- (at t = 0) (ψ_o), maximum

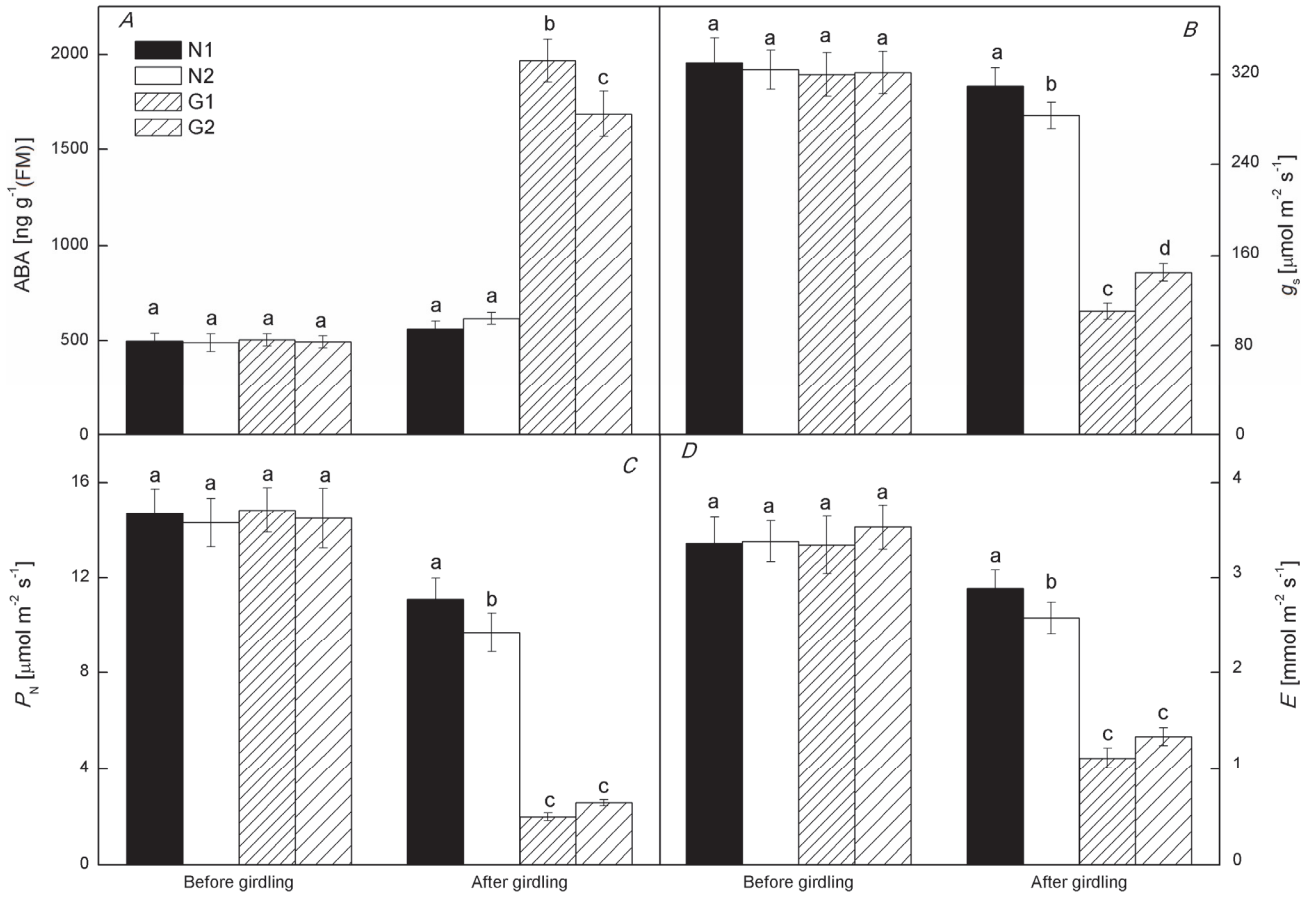

Fig. 3. ABA content, g_s, P_N, and E of *Alhagi sparsifolia* under N1, N2, G1, and G2 treatment. *A*: ABA content, *B*: g_s, *C*: P_N, *D*: E of *A. sparsifolia* before and after girdling. ABA – abscisic acid; g_s – stomatal conductance; P_N – net photosynthesis rate; E – transpiration rate. *Different letters* indicate significant difference (p<0.05). The data represent means of five biological replicates ± SD. N1 – nongirdling with one branch left; G1 – girdling with one branch left; N2 – nongirdling with two branches left; G2 – girdling with two branches left.

quantum yield for primary photochemistry (φ_{Po}), performance index on absorption basis (PI_{abs}), trapped energy flux per reaction center (TR_o/RC), electron transport flux per reaction center (ET_o/RC), and density of RCs (Q_A^- reducing PSII reaction centers) (RC/CS) were lowered in the order of N1 > N2 > G2 > G1 (Fig. 7, Table 1S). The results showed that girdling significantly increased M_o, ABS/RC, and DI_o/RC, and decreased S_m, φ_{Eo}, ψ_o, φ_{Po}, PI_{abs} (Fig. 7), TR_o/RC, ET_o/RC, and RC/CS (Table 1S). Similar to the indicators described above, changes of these Chl fluorescence parameters also appeared to be mitigated when the intact branch was present on the root system connected also to the girdled branch. Inhibition of root respiration also showed a similar effect on Chl fluorescence parameters in *A. sparsifolia* leaf as the effect of girdling, although the degree was much smaller. M_o (Fig. 7), ABS/RC, and DI_o/RC (Table 1S) increased by 10.0, 16.4, and 54.7%, respectively, in the N2 treatment compared with N1, while S_m, φ_{Eo}, ψ_o, φ_{Po}, PI_{abs} (Fig. 7), TR_o/RC, ET_o/RC, and RC/CS (Table 1S) decreased by 10.7, 9.4, 12.9, 9.0, 11.8, 4.2, 3.8, and 10.6%, respectively, in the N2 treatment compared with N1. From the fluorescence kinetic curve, no obvious K-points were found in the fluorescence curves for the treatments before girdling, indicating a typical OJIP phase. After 30 d from girdling, the fluorescence intensity in G1 and G2 was far smaller than that of the N1 and N2 treatments; the fluorescent intensity was in order of N1 > N2 > G2 > G1. In addition, the obvious K-point occurred after G1 and G2, at about 0.3 ms. However, at the same time, no obvious K-point was observed in Chl *a* fluorescence kinetics for the N1 and N2 treatments (Fig. 8).

Discussion

Our study provided evidence that root respiration is associated with leaf senescence. Although inhibition of root respiration in the girdling system might not be the only cause of leaf senescence, it obviously accelerated it.

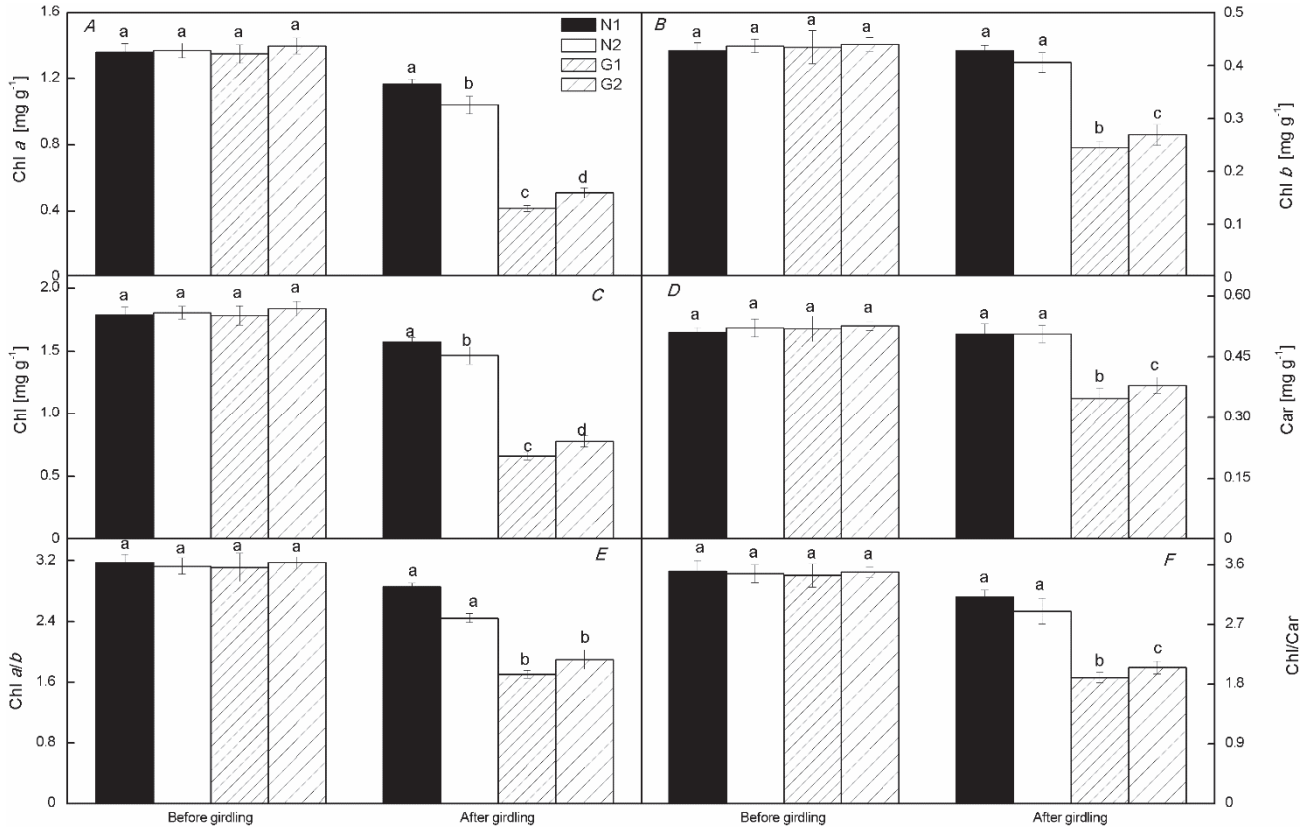

Fig. 4. Pigment contents and ratios of *Alhagi sparsifolia* under N1, N2, G1, and G2 treatment. *A*: Chl *a* content, *B*: Chl *b* content, *C*: Chl (*a*+*b*) content, *D*: Car content, *E*: Chl *a*/*b*, *F*: Chl/Car. *Different letters* indicate significant difference (p<0.05). The data represent means of five biological replicates ± SD. N1 – nongirdling with one branch left; G1 – girdling with one branch left; N2 – nongirdling with two branches left; G2 – girdling with two branches left.

Moreover, the difference between G1 and G2 was greater than that between N1 and N2, suggesting that in girdled branches, root respiration-related leaf senescence was more induced compared with normal branches.

Girdling disrupted the basipetal movement of photosynthetic products through the phloem, which resulted in the build-up of carbohydrates on the side of the girdle closest to the source(s) of metabolites, and in a reduction in tissue on the opposite side of the girdle (Rivas *et al.* 2006, Urban and Alphonsout 2007, Yang *et al.* 2013, Bloemen *et al.* 2014). In this situation, carbohydrates always accumulated not only in phloem above the girdle but also in leaves (Li *et al.* 2003, Peuke *et al.* 2006) which always leads to the end-product inhibition of P_N (Goldschmidt and Huber 1992, Nebauer *et al.* 2011, Nikinmaa *et al.* 2013) and carbon feast-induced leaf senescence (Parrott *et al.* 2005, Tang *et al.* 2016). On the root side, carbohydrates decline because of the interruption of their flow to belowground tissues (Frey *et al.* 2006, Bloemen *et al.* 2014). It is assumed to be the reason for the subsequent decline in root respiration (Högberg *et al.* 2001, 2009, Olsson *et al.* 2005, Frey *et al.* 2006, Bloemen *et al.* 2014). Our study revealed that girdling increased leaf soluble sugars and starch, and decreased root soluble sugars and starch, which might be the reason for the decline of root respiration (Fig. 2). This result is consistent with the previous studies described above (Högberg *et al.* 2001, 2009, Olsson *et al.* 2005, Frey *et al.* 2006, Bloemen *et al.* 2014). Interestingly, the root respiration was lowered in order: N1 > N2 (G2) > G1, which is consistent with the carbohydrate (soluble sugar and starch) content in roots (Fig. 2). Thus, when both the girdled and nongirdled branches were connected on the same roots (N2, G2), the root respiration was between the single girdling (G1) and single nongirdling (N1) treatment.

Both ABA and carbohydrates are transported in a similar manner in phloem (Nikinmaa *et al.* 2013); thus, in addition to carbohydrate build-up, girdling also leads to ABA accumulation in leaves (Rivas *et al.* 2011). The reason for this might be the disruption of ABA flow from leaves to roots through phloem (Setter *et al.* 1980). Previous study also showed that ABA showed a strong relationship with carbohydrates; ABA concentration affects leaf carbohydrate metabolism (Wang *et al.* 2012). The present study demonstrated that girdling resulted in the accumulation of ABA in leaves because both G1 and G2 showed the high ABA content compared with N1 and N2, respectively (Fig. 3). The ABA content is closely

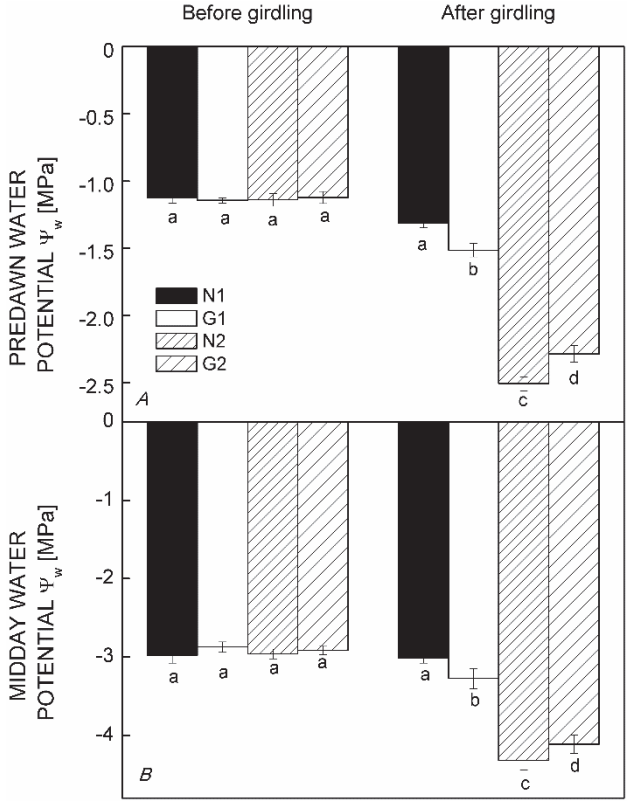

Fig. 5. Predawn water potential (Ψ_w, *A*) and midday Ψ_w (*B*) of *Alhagi sparsifolia* under N1, N2, G1, and G2 treatment. *Different letters* indicate significant difference ($p<0.05$). The data represent means of five biological replicates ± SD. N1 – nongirdling with one branch left; G1 – girdling with one branch left; N2 – nongirdling with two branches left; G2 – girdling with two branches left.

connected to changes of g_s (Speirs *et al.* 2013) and previous studies have shown that ABA accumulation in girdled leaves subsequently led to the decline of g_s, and thus to the decline of P_N (Setter *et al.* 1980). This was also proven in our study because both g_s and P_N in girdled (G1, G2) leaves showed the significant decline along with the increase of the ABA content (Fig. 3).

Decline of *E* in girdled (G1, G2) leaves might occur due to the reduction of g_s (Bouranis *et al.* 2014), which is consistent with previous research showing that the decrease of g_s, which resulted from phloem girdling, led subsequently to the reduction of *E* (Williams *et al.* 2000). The ABA content was higher in G1 than in G2, and was also higher in N2 than in N1 (Fig. 3). These results suggested that the ABA content in leaves was associated with root respiration, because root respiration in G2 (N2) was lower than that in G1, and the content of ABA in N2 (G2) was higher compared to N1 (Fig. 2). This study implied that high root respiration was associated with the low ABA content, and thus the g_s, P_N, and *E* in G1 were lower in comparison with G2, and in N2 were lower in comparison with N1 (Fig. 3).

Previous studies also demonstrated that ABA is always associated with the leaf senescence process (Kumar *et al.* 2014). Moreover, MDA together with Chl content and P_N has been used as a useful indication of leaf senescence (Dong *et al.* 2008, Dai and Dong 2011). Therefore, in addition to P_N, we also measured the Chl and MDA content for leaf senescence study after the treatments (N1, G1, N2, and G2).

In our study, Chl *a*, Chl *b*, and Chl (*a*+*b*) content was lower in the girdled (G1, G2) leaves compared with non-girdled ones (N1, N2) (Fig. 4), while the MDA content in girdled (G1, G2) leaves was higher than that in nongirdled (N1, N2) leaves. This result is consistent with previous studies which showed that girdling induced the decline of the Chl content and increased the MDA content (Dai and Dong 2011). It suggested that girdling-induced leaf senescence is consistent with previous studies (Parrott *et al.* 2007, Dai and Dong 2011).

Moreover, this might result from ABA accumulation (Fig. 3) and carbohydrate build-up (Fig. 2) in leaves, which has also been demonstrated by previous studies (Figs. 2, 3) (Parrott *et al.* 2005, Dai and Dong 2011). The Chl content was higher in N1 than that in N2 and was lower in G1 than that in G2 (just the opposite that of the MDA content) (Fig. 4). This result implied that the acceleration of leaf senescence in N2 (compared with N1) and G1 (compared with G2) were induced by inhibition of root respiration.

Some studies showed that the Chl *a*/*b* ratio exhibited no decline during autumnal leaf senescence (Adams *et al.* 1990), while in other studies, the Chl *a*/*b* ratio in leaves declined significantly during senescence (Agüera *et al.* 2012). Interestingly, both courses can be found in our study. Compared with nongirdled (N1, N2) leaves, the girdled (G1, G2) leaves showed a significant decline; however, although N2 (compared with N1) and G1 (compared with G2) showed obvious leaf senescence, the Chl *a*/*b* ratio changed only a little (Fig. 4*E*). The Chl *a*/*b* characteristic indicated that leaf senescence was a highly controlled process during root respiration inhibition-induced senescence, similar to the previously shown natural senescence (Adams *et al.* 1990). However, girdling-induced senescence might disturb this control mechanism.

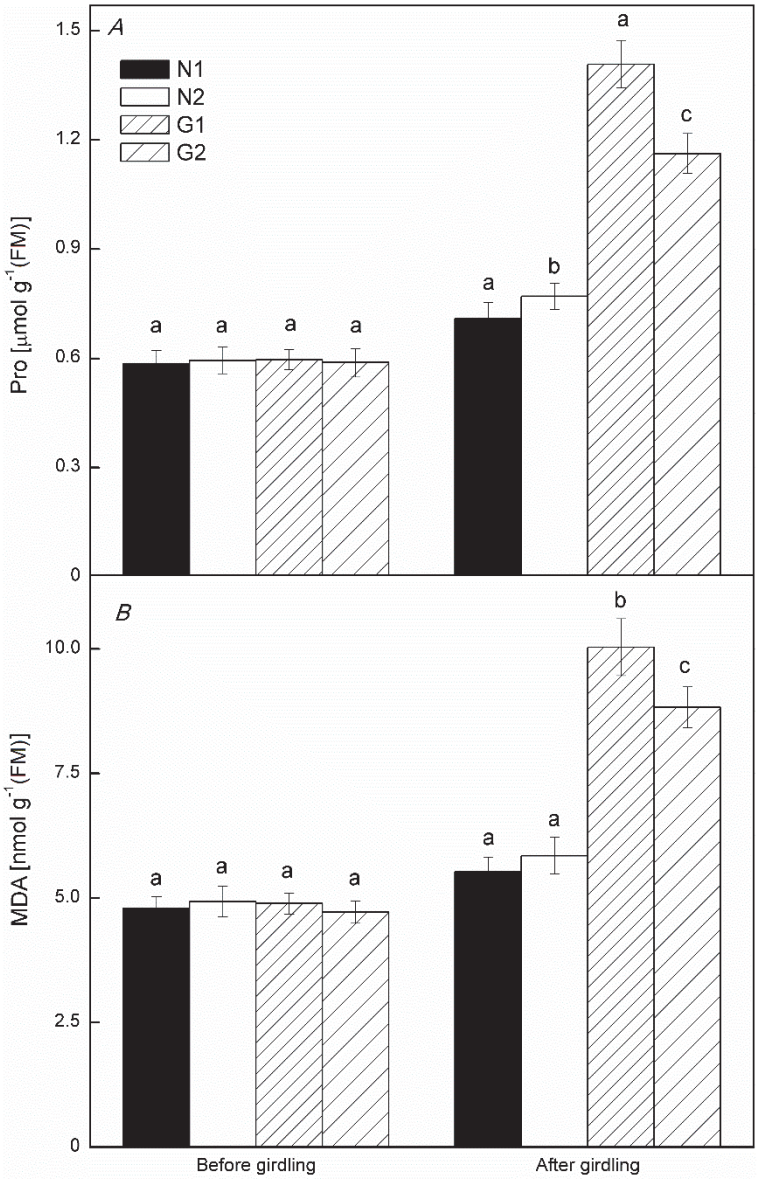

Fig. 6. Proline (Pro, *A*) and malondialdehyde (MDA, *B*) contents of *Alhagi sparsifolia* under N1, N2, G1, and G2. FM – fresh mass. *Different letters* indicate significant difference (p<0.05). The data represent means of five biological replicates ± SD. N1 – nongirdling with one branch left; G1 – girdling with one branch left; N2 – nongirdling with two branches left; G2 – girdling with two branches left.

In addition, our study found that inhibition of root respiration led to the decline of water potential, and the decrease of Ψ_P and Ψ_M in N2 (compared with N1) and G1 (compared with G2), which is consistent with the results of root respiration inhibition in N2 (compared with N1) and G1 (compared with G2) (Fig. 5*A*,*B*). The Pro content increased in N2 (compared with N1) and G1 (compared with G2) which indicated water stress in N2 (compared with N1) and G1 (compared with G2) (Fig. 6*A*), and might be the reason for root respiration-induced leaf senescence (Tschaplinski and Blake 1985). Previous studies demonstrated that girdling reduced a root carbohydrate content (Roper and Williams 1989) and root respiration (Fumuro 1998, Högberg *et al.* 2001), thus leading to the reduction of water absorption (Fumuro1998). Our study also revealed that girdling induced a decline of Ψ_{leaf} which might occur due to the reduction of water absorption; inhibition of root respiration might play a key role because one of the critical functions of roots is to absorb water.

Our study described fast Chl fluorescence induction kinetic curve for different types of leaf senescence. In the present study, the rate of leaf senescence in the treatments declined in order of G1 > G2 > N2 > N1. Leaf senescence induced degradation of protein D1, which caused block of electron transport, especially decrease Q_B exchanges from the plastoquinone pool. This led to the inhibition of acceptor capacity, manifested as decreased S_m (Fig. 7*B*). This resulted in the inhibition of the electron acceptor sink capacity (S_m) of the PSII acceptor side; there was an increased probability that a trapped exciton moves an electron into the electron transport chain beyond Q_A^- (ψ_o), reducing the quantum yield for electron transport (φ_{Eo})

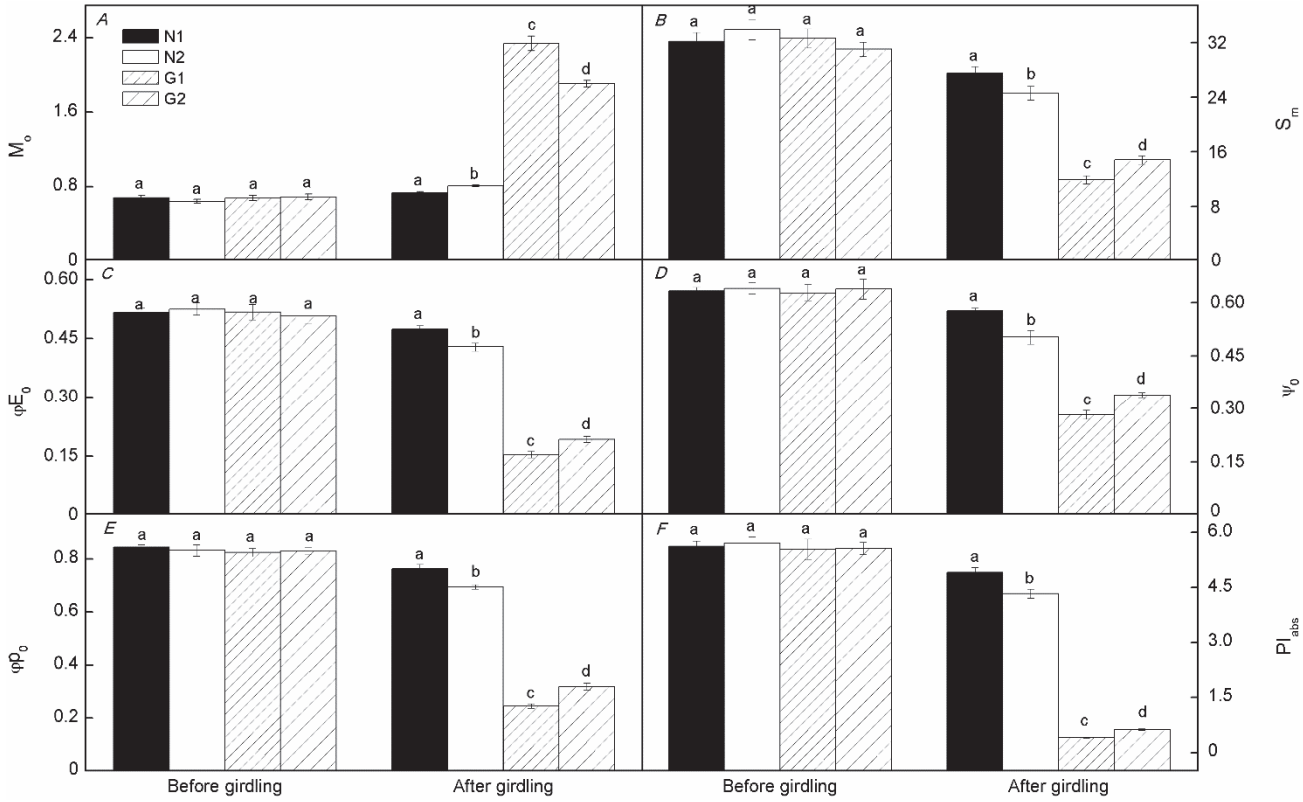

Fig. 7. M_o, S_m, φ_{Eo}, ψ_o, φ_{po}, and PI_{abs} of *Alhagi sparsifolia* under N1, N2, G1, and G2 treatment. M_o – approximated initial slope of the fluorescence transient; S_m – normalised total complementary area above the OJIP transients (reflecting single-turnover Q_A reduction events); φ_{Eo} – quantum yield for electron transport (at t = 0); ψ_o – probability that a trapped exciton moves an electron into the electron transport chain beyond Q_A^- (at t = 0); φ_{Po} – maximum quantum yield for primary photochemistry (at t = 0); PI_{abs} – performance index on absorption basis. *Different letters* indicate a significant difference (p<0.05). The data represent means of five biological replicates ± SD. N1 – nongirdling with one branch left; G1 – girdling with one branch left; N2 – nongirdling with two branches left; G2 – girdling with two branches left.

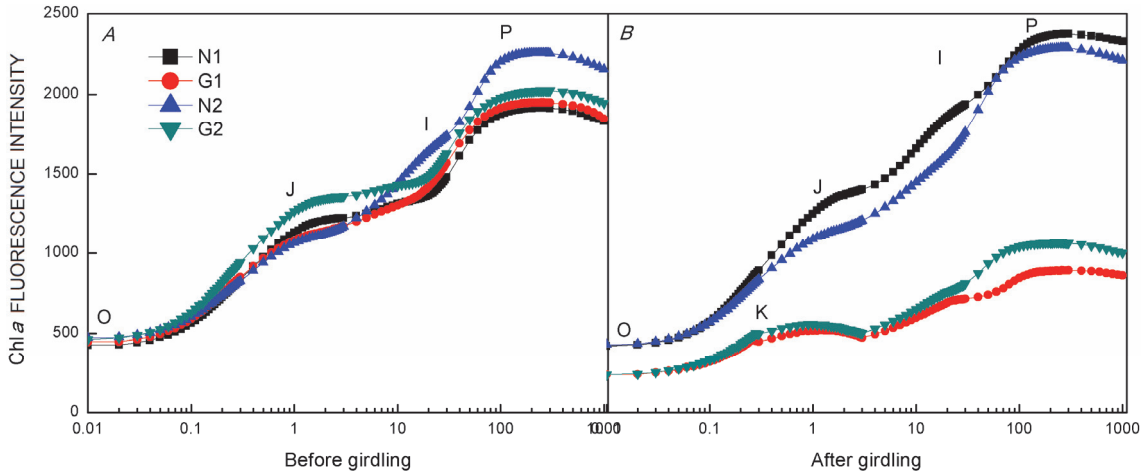

Fig. 8. OJIP chlorophyll (Chl) *a* fluorescence transient curves (log time scale) in *Alhagi sparsifolia* in the four treatments (N1, G1, N2, and G2) before (*A*) and after (*B*) girdling. N1 – nongirdling with one branch left; G1 – girdling with one branch left; N2 – nongirdling with two branches left; G2 – girdling with two branches left.

(Fig. 7*C*,*D*). More energy was used to restore Q_A, accelerating Q_A reduction (M_o), shown as an increase in M_o (Fig. 7*A*). The change of these fluorescence parameters indicated that leaf senescence led to inhibition on the acceptor side of PSII and this inhibition was much greater in plants with girdling-induced senescence than in those

with root respiration inhibition-induced senescence.

Some previous studies demonstrated that the maximum photochemical efficiency (φ_{Po}) changed very little during leaf senescence (Adams *et al.* 1990, Lu *et al.* 2002), while other studies showed that leaf senescence induced φ_{Po} (F_v/F_m) decline (Mikkelsen and Heide-Jørgensen 1996, Song *et al.* 1997). Our study revealed that both girdling- and root respiration inhibition-induced senescence led to the decline of φ_{Po}, when φ_{Po} in nongirdled (N1, N2) plants was lower compared with φ_{Po} in girdled (G1, G2) leaves (Fig. 7*A*), and φ_{Po} was much lower in N2 (compared with N1) and G1 (compared with G2). PI_{abs} includes three parameters (RC/ABS, φ_{Po}, and ψ_o) and reflects the performance and state of photosynthetic apparatus, which is similar to φ_{Po}. However, compared with φ_{Po}, PI_{abs} is more sensitive and can better reflect the impact of stress on the photosynthetic apparatus (Appenroth *et al.* 2001, van Heerden *et al.* 2004). In our study, the change of PI_{abs} after four treatments (N1, G1, N2, and G2) was similar to the change of φ_{Po}, although PI_{abs} changed more during the senescence process (Fig. 7*F*). Thus, PI_{abs} may be a better parameter to reflect the change of PSII in senescence compared with φ_{Po}.

Previous studies have demonstrated that when the donor side of PSII was damaged, the intensity of Chl fluorescence increased after a very short period of time (before J point), and K-phase appeared (a characteristic loci of about 300 μs after illumination) (Srivastava *et al.* 1997). The emergence of K-phase was caused by the inhibition of the water-splitting system and the partial inhibition of the acceptor side before Q_A (Strasser *et al.* 2000, 2004). The appearance of the K-phase can be specifically attributed to damage on the donor side, especially indicating that the oxygen-evolving complex (OEC) was affected (Strasser 1997). In the present study, the K-phase appeared at the girdled (G1, G2) leaves, whereas, in the non-girdled (N1, N2) leaves (Fig. 8*B*), no K-phase was found. This study suggested that girdling-induced senescence resulted in damage of OEC, while root respiration inhibition-induced senescence did not lead to damage of OEC. Our study also implied that although the inhibition of root respiration can induce leaf senescence, this senescence was a highly regulated process which may be genetically controlled, and thus maintain the cell structure and function in a stable condition. In this aspect, it is quite similar to natural senescence (Adams *et al.* 1990). However, girdling-induced senescence might disturb such a regulation, which may lead to the deterioration of cell structure and function, especially of the photosynthetic apparatus. This was shown as the decline of Chl *a*/*b* and the appearance of the K-phase in girdled (G1, G2) leaves (Figs. 4*E*, 8*B*).

In our study, leaf senescence (both girdling-induced and root respiration inhibition-induced) led to the decrease of active reaction centers per unit area (RC/CS), which subsequently resulted in the increase in the energy absorbed by the unit of reaction center (ABS/RC) (Table 1S). Although the absorbed energy (ABS/RC) increased, it did not lead to the increase of captured energy (TR_o/RC). In contrast, TR_o/RC declined during senescence, followed by a decline of electron transport-inactive RC (ET_o/RC). This led to a dissipation of most of the energy absorbed by reaction centers (RC) as thermal energy or fluorescence, showing as increasing of effective dissipation of active RC (DR_o/RC) (Table 1S). Since it is known that the initiation of nonphotochemical quenching (thermal and fluorescence) requires more time than photosynthetic electron transfer (Krause and Weis 1991), the increasing of nonphotochemical quenching in senescent leaves may produce more reactive oxygen species in PSII. In order to mitigate the stress of reactive oxygen, plants save more Car compared to Chl during leaf senescence, which was shown as the decline of Chl/Car during senescence (Fig. 4*F*). However, the total Car content declined with leaf senescence, because Car can act as accessory light-harvesting pigments, and the decline of Car content leads to the reduction of absorbed energy in RC. This may constitute another way how to relieve excitation pressure in the RC and prevent excessive reactive oxygen. Thus, Car may play a key photoprotective role in leaf senescence, which was proven by previous studies (Merzlyak and Solovchenko 2002).

Overall, our study proved that root respiration is related to leaf senescence, and that inhibition of root respiration constituted another factor in leaf senescence in addition to ABA build-up and carbohydrate accumulation in girdled leaves. The mechanism for root respiration inhibition-induced leaf senescence might reside in the decline of water absorbed by roots, thus leading to water stress in leaves and leaf senescence. In addition, root respiration-induced leaf senescence was a highly regulated process, genetically controlled. Our study helped elucidate the relationship between leaf senescence and root respiration and find the possible mechanism for root respiration inhibition-induced senescence. However, our study only explored one possible mechanism for root respiration inhibition-induced senescence. Additional studies should be conducted to explore other mechanisms. Moreover, measuring the water absorption rate and plant hydraulic properties may yield particularly valuable insights.

References

Adams W.W., Winter K., Schreiber U. *et al.*: Photosynthesis and chlorophyll fluorescence characteristics in relationship to changes in pigment and element composition of leaves of *Platanus occidentalis* L. during autumnal leaf senescence. – Plant Physiol. **92**: 1184-1190, 1990.

Agüera E., Molina E., de la Mata L. *et al.*: Metabolic Regulation of Leaf Senescence in Sunflower (*Helianthus annuus* L.) Plants. – In: Nagata T. (ed.): Senescence. Pp. 51-68. InTech,

Rijeka 2012.
Appenroth K-J., Stöckel J., Srivastava A. *et al.*: Multiple effects of chromate on the photosynthetic apparatus of *Spirodela polyrhiza* as probed by OJIP chlorophyll a fluorescence measurements. – Environ. Pollut. **115**: 49-64, 2001.
Besseau S., Li J., Palva E.T.: WRKY54 and WRKY70 co-operate as negative regulators of leaf senescence in *Arabidopsis thaliana*. – J. Exp. Bot. **63**: 2667-2679, 2012.
Bhupinderpal-Singh, Nordgren A., Ottosson Löfvenius M., Högberg M. *et al.*: Tree root and soil heterotrophic respiration as revealed by girdling of boreal Scots pine forest: extending observations beyond the first year. – Plant Cell Environ. **26**: 1287-1296, 2003.
Bloemen J., Agneessens L., van Meulebroek L. *et al.*: Stem girdling affects the quantity of CO_2 transported in xylem as well as CO_2 efflux from soil. – New Phytol. **201**: 897-907, 2014.
Bouranis D.L., Dionias A., Chorianopoulou S.N. *et al.*: Distribution profiles and interrelations of stomatal conductance, transpiration rate and water dynamics in young maize laminas under nitrogen deprivation. – Am. J. Plant Sci. **5**: 659-670, 2014.
Brouquisse R., Masclaux C., Feller U. *et al.*: Protein hydrolysis and nitrogen remobilisation in plant life and senescence. – In: Lea P.J., Morot-Gaudry J.-F. (ed.): Plant Nitrogen. Pp. 275-293. Springer-Verlag, Berlin 2001.
Buchanan-Wollaston V., Page T., Harrison E. *et al.*: Comparative transcriptome analysis reveals significant differences in gene expression and signalling pathways between developmental and dark/starvation – induced senescence in *Arabidopsis*. – Plant J. **42**: 567-585, 2005.
Chen Y., Hou M., Liu L. *et al.*: The Maize *DWARF1* encodes a gibberellin 3-oxidase and is dual localized to the nucleus and cytosol. – Plant Physiol. **166**: 2028-2039, 2014.
Dai J., Dong H.: Stem girdling influences concentrations of endogenous cytokinins and abscisic acid in relation to leaf senescence in cotton. – Acta Physiol. Plant. **33**: 1697-1705, 2011.
Demiral T., Türkan I.: Comparative lipid peroxidation, antioxidant defense systems and proline content in roots of two rice cultivars differing in salt tolerance. – Environ. Exp. Bot. **53**: 247-257, 2005.
Dong H., Niu Y., Li W. *et al.*: Effects of cotton rootstock on endogenous cytokinins and abscisic acid in xylem sap and leaves in relation to leaf senescence. – J. Exp. Bot. **59**: 1295-1304, 2008.
Frey B., Hagedorn F., Giudici F.: Effect of girdling on soil respiration and root composition in a sweet chestnut forest. – Forest Ecol. Manage. **225**: 271-277, 2006.
Fu W., Li P., Wu Y. *et al.*: Effects of different light intensities on anti-oxidative enzyme activity, quality and biomass in lettuce. – Hort. Sci. **39**: 129-134, 2012.
Fukao T., Yeung E., Bailey-Serres J. *et al.*: The submergence tolerance gene SUB1A delays leaf senescence under prolonged darkness through hormonal regulation in rice. – Plant Physiol. **160**: 1795-1807, 2012.
Fumuro M. *et al.*: Effects of trunk girdling during early shoot elongation period on tree growth, mineral absorption, water stress, and root respiration in Japanese persimmon (*Diospyros kaki* L.) cv. Nishimurawase. – J. Jpn. Soc. Hortic. Sci. **67**: 219-227, 1998.
Goldschmidt E.E., Huber S.C.: Regulation of photosynthesis by end-product accumulation in leaves of plants storing starch, sucrose, and hexose sugars. – Plant Physiol. **99**: 1443-1448, 1992.
Gregersen P.L., Culetic A., Boschian L. *et al.*: Plant senescence and crop productivity. – Plant Mol. Biol. **82**: 603-622, 2013.
Högberg P., Bhupinderpal-Singh, Löfvenius M.O., Nordgren A.: Partitioning of soil respiration into its autotrophic and heterotrophic components by means of tree-girdling in old boreal spruce forest. – Forest Ecol. Manage. **257**: 1764-1767, 2009.
Högberg P., Nordgren A., Buchmann N. *et al.*: Large-scale forest girdling shows that current photosynthesis drives soil respiration. – Nature **411**: 789-792, 2001.
Hopkins M., Taylor C., Liu Z. *et al.*: Regulation and execution of molecular disassembly and catabolism during senescence. – New Phytol. **175**: 201-214, 2007.
Jiang Y., Liang G., Yang S. *et al.*: *Arabidopsis* WRKY57 functions as a node of convergence for jasmonic acid- and auxin-mediated signaling in jasmonic acid-induced leaf senescence. – Plant Cell **26**: 230-245, 2014.
Johnsen K., Maier C., Sanchez F. *et al.*: Physiological girdling of pine trees *via* phloem chilling: proof of concept. – Plant Cell Environ. **30**: 128-134, 2007.
Koeslin-Findeklee F., Meyer A., Girke A. *et al.*: The superior nitrogen efficiency of winter oilseed rape (*Brassica napus* L.) hybrids is not related to delayed nitrogen starvation-induced leaf senescence. – Plant Soil **384**: 347-362, 2014.
Kong L., Si J., Sun M. *et al.*: Deep roots are pivotal for regulating post-anthesis leaf senescence in wheat (*Triticum aestivum* L.). – J. Agron. Crop Sci. **199**: 209-216, 2013.
Kotakis C., Kyzeridou A., Manetas Y. *et al.*: Photosynthetic electron flow during leaf senescence: Evidence for a preferential maintenance of photosystem I activity and increased cyclic electron flow. – Photosynthetica **52**: 413-420, 2014.
Krause G., Weis E.: Chlorophyll fluorescence and photosynthesis: the basics. – Annu. Rev. Plant Biol. **42**: 313-349, 1991.
Kumar M., Singh V.P., Arora A. *et al.*: The role of abscisic acid (ABA) in ethylene insensitive Gladiolus (*Gladiolus grandiflora Hort*.) flower senescence. – Acta Physiol. Plant. **36**: 151-159, 2014.
Li C.Y., Weiss D., Goldschmidt E.E.: Girdling affects carbohydrate-related gene expression in leaves, bark and roots of alternate-bearing citrus trees. – Ann. Bot.-London **92**: 137-143, 2003.
Li N., Zhang S., Zhao Y. *et al.*: Over-expression of AGPase genes enhances seed weight and starch content in transgenic maize. – Planta **233**: 241-250, 2011.
Lichtenthaler H.K.: Chlorophylls and carotenoids: Pigments of photosynthetic biomembranes. – Methods Enzymol. **148**: 350-382, 1987.
Lim P.O., Kim H.J., Nam H.G.: Leaf senescence. – Annu. Rev. Plant Biol. **58**: 115-136, 2007.
Liu B., Zeng F.J., Arndt S.K. *et al.*: Patterns of root architecture adaptation of a phreatophytic perennial desert plant in a hyperarid desert. – S. Afr. J. Bot. **86**: 56-62, 2013.
Lobell D.B., Sibley A., Ortiz-Monasterio J.I.: Extreme heat effects on wheat senescence in India. – Nature Climate Change **2**: 186-189, 2012.
Lu Q., Lu C., Zhang J. *et al.*: Photosynthesis and chlorophyll *a* fluorescence during flag leaf senescence of field-grown wheat plants. – J. Plant Physiol. **159**: 1173-1178, 2002.
Merzlyak M.N., Solovchenko A.E.: Photostability of pigments in ripening apple fruit: a possible photoprotective role of

carotenoids during plant senescence. – Plant Sci. **163**: 881-888, 2002.

Mikkelsen T.N., Heide-Jørgensen H.S.: Acceleration of leaf senescence in *Fagus sylvatica* L. by low levels of tropospheric ozone demonstrated by leaf colour, chlorophyll fluorescence and chloroplast ultrastructure. – Trees **10**: 145-156, 1996.

Mittler R., Merquiol E., Hallak-Herr E. *et al.*: Living under a 'dormant'canopy: a molecular acclimation mechanism of the desert plant Retama raetam. – The Plant Journal **25**: 407-416, 2001.

Moore B., Zhou L., Rolland F. *et al.*: Role of the *Arabidopsis* glucose sensor HXK1 in nutrient, light, and hormonal signaling. – Science **300**: 332-336, 2003.

Nebauer S.G., Renau-Morata B., Guardiola J.L. *et al.*: Photosynthesis down-regulation precedes carbohydrate accumulation under sink limitation in Citrus. – Tree Physiol. **31**: 169-177, 2011.

Nikinmaa E., Hölttä T., Hari P. *et al.*: Assimilate transport in phloem sets conditions for leaf gas exchange. – Plant Cell Environ. **36**: 655-669, 2013.

Noodén L.D., Guiamét J.J., John I.: Senescence mechanisms. – Physiol. Plantarum **101**: 746-753, 1997.

Olsson P., Linder S., Giesler R. *et al.*: Fertilization of boreal forest reduces both autotrophic and heterotrophic soil respiration. – Glob. Change Biol. **11**: 1745-1753, 2005.

Parrott D., Yang L., Shama L. *et al.*: Senescence is accelerated, and several proteases are induced by carbon "feast" conditions in barley (*Hordeum vulgare* L.) leaves. – Planta **222**: 989-1000, 2005.

Parrott D.L., Martin J.M., Fischer A.M.: Analysis of barley (*Hordeum vulgare*) leaf senescence and protease gene expression: a family C1A cysteine protease is specifically induced under conditions characterized by high carbohydrate, but low to moderate nitrogen levels. – New Phytol. **187**: 313-331, 2010.

Parrott D.L., McInnerney K., Feller U. *et al.*: Steam-girdling of barley (*Hordeum vulgare*) leaves leads to carbohydrate accumulation and accelerated leaf senescence, facilitating transcriptomic analysis of senescence-associated genes. – New Phytol. **176**: 56-69, 2007.

Peuke A.D., Windt C., Van As H.: Effects of cold-girdling on flows in the transport phloem in *Ricinus communis*: is mass flow inhibited? – Plant Cell Environ **29**: 15-25, 2006.

Pourtau N., Jennings R., Pelzer E. *et al.*: Effect of sugar-induced senescence on gene expression and implications for the regulation of senescence in *Arabidopsis*. – Planta **224**: 556-568, 2006.

Rahman M.M., Chongling Y., Rahman M.M. *et al.*: Effects of copper on growth, accumulation, antioxidant activity and malondialdehyde content in young seedlings of the mangrove species *Kandelia candel* (L.). – Plant Biosyst. **146**: 47-57, 2012.

Rivas F., Erner Y., Alós E. *et al.*: Girdling increases carbohydrate availability and fruit-set in citrus cultivars irrespective of parthenocarpic ability. – J. Hortic. Sci. Biotech. **81**: 289-295, 2006.

Rivas F., Fornes F., Rodrigo M. *et al.*: Changes in carotenoids and ABA content in Citrus leaves in response to girdling. – Sci. Hortic.-Amsterdam **127**: 482-487, 2011.

Robert-Seilaniantz A., Grant M., Jones J.D.: Hormone crosstalk in plant disease and defense: more than just jasmonate-salicylate antagonism. – Annu. Rev. Phytopathol. **49**: 317-343, 2011.

Roberts I.N., Caputo C., Criado M.V. *et al.*: Senescence-associated proteases in plants. – Physiol. Plantarum. **145**: 130-139, 2012.

Roper T.R., Williams L.E.: Net CO_2 assimilation and carbohydrate partitioning of grapevine leaves in response to trunk girdling and gibberellic acid application. – Plant Physiol. **89**: 1136-1140, 1989.

Sakuraba Y., Schelbert S., Park S.Y. *et al.*: STAY-GREEN and chlorophyll catabolic enzymes interact at light-harvesting complex II for chlorophyll detoxification during leaf senescence in *Arabidopsis*. – Plant Cell **24**: 507-518, 2012.

Setter T.L., Brun W.A., Brenner M.L.: Effect of obstructed translocation on leaf abscisic acid, and associated stomatal closure and photosynthesis decline. – Plant Physiol. **65**: 1111-1115, 1980.

Sitton D., Itai C., Kende H.: Decreased cytokinin production in the roots as a factor in shoot senescence. – Planta **73**: 296-300, 1967.

Song J., Deng W., Beaudry R.M. *et al.*: Changes in chlorophyll fluorescence of apple fruit during maturation, ripening, and senescence. – HortSci. **32**: 891-896, 1997.

Speirs J., Binney A., Collins M. *et al.*: Expression of ABA synthesis and metabolism genes under different irrigation strategies and atmospheric VPDs is associated with stomatal conductance in grapevine (*Vitis vinifera* L. cv Cabernet Sauvignon). – J. Exp. Bot. **64**: 1907-1916, 2013.

Sperotto R.A., Boff T., Duarte G.L. *et al.*: Increased senescence-associated gene expression and lipid peroxidation induced by iron deficiency in rice roots. – Plant Cell Rep. **27**: 183-195, 2008.

Srivastava A., Guissé B., Greppin H.: *et al.*: Regulation of antenna structure and electron transport in photosystem II of *Pisum sativum* under elevated temperature probed by the fast polyphasic chlorophyll *a* fluorescence transient: OKJIP. – BBA-Bioenergetics **1320**: 95-106, 1997.

Strasser B.J.: Donor side capacity of photosystem II probed by chlorophyll *a* fluorescence transients. – Photosynth. Res. **52**: 147-155, 1997.

Strasser R.J., Srivastava A., Tsimilli-Michael M.: The fluorescence transient as a tool to characterize and screen photosynthetic samples. – In: Yunus M. (ed.): Probing Photosynthesis: Mechanisms, Regulation and Adaptation. Pp. 445-483. Taylor & Francis, London, 2000.

Strasser R.J., Tsimilli-Michael M., Srivastava A.: Analysis of the chlorophyll *a* fluorescence transient. – In: Papageorgiou G., Govindjee (ed.): Advances in Photosynthesis and Respiration. Chlorophyll Fluorescence a Signature of Photosynthesis. Pp. 321-362. Kluwer, Dordrecht 2004.

Subke J.A., Hahn V., Battipaglia G. *et al.*: Feedback interactions between needle litter decomposition and rhizosphere activity. – Oecologia **139**: 551-559, 2004.

Tang G.L., Li X.Y., Lin L.S. *et al.*: Combined effects of girdling and leaf removal on fluorescence characteristic of *Alhagi Sparsifolia* leaf senescence. – Plant Biol. **17**: 980-989, 2015a.
Tang G.L., Li X.Y., Lin L.S. *et al.*: Girdling-induced *Alhagi sparsifolia* senescence and chlorophyll fluorescence changes. – Photosynthetica **53**: 585-596, 2015b.

Tang G.L., Li X.Y., Lin L.S. *et al.*: Impact of girdling and leaf removal on *Alhagi sparsifolia* leaf senescence. – Plant Growth Regul. **78**: 205-216, 2016.

Tschaplinski T.J., Blake T.J.: Effects of root restriction on growth correlations, water relations and senescence of alder seedlings. – Physiol. Plantarum **64**: 167-176, 1985.

Urban L., Alphonsout L.: Girdling decreases photosynthetic electron fluxes and induces sustained photoprotection in mango leaves. – Tree Physiol. **27**: 345-352, 2007.

van Heerden P.D., Strasser R.J., Krüger G.H.: Reduction of dark chilling stress in N_2–fixing soybean by nitrate as indicated by chlorophyll *a* fluorescence kinetics. – Physiol. Plantarum **121**: 239-249, 2004.

Veselov D.S., Sharipova G.V., Veselov S.U. *et al.*: The effects of NaCl treatment on water relations, growth, and ABA content in barley cultivars differing in drought tolerance. – J. Plant Growth Regul. **27**: 380-386, 2008.

Vogelmann K., Drechsel G., Bergler J. *et al.*: Early senescence and cell death in *Arabidopsis* saul1 mutants involves the PAD4-dependent salicylic acid pathway. – Plant Physiol. **159**: 1477-1487, 2012.

Vysotskaya L., Kudoyarova G., Veselov S. *et al.*: Unusual stomatal behaviour on partial root excision in wheat seedlings. – Plant Cell Environ. **27**: 69-77, 2004.

Wang S., Hu L., Sun J. *et al.*: Effects of exogenous abscisic acid on leaf carbohydrate metabolism during cucumber seedling dehydration. – Plant Growth Regul. **66**: 87-93, 2012.

Williams L.E., Araujo F.J.: Correlations among predawn leaf, midday leaf, and midday stem water potential and their correlations with other measures of soil and plant water status in *Vitis vinifera*. – J. Am. Soc. Hortic. Sci. **127**: 448-454, 2002.

Williams L.E., Baeza P., Vaughn P. *et al.*: Midday measurements of leaf water potential and stomatal conductance are highly correlated with daily water use of Thompson Seedless grapevines. – Irrigation Sci. **30**: 201-212, 2012.

Williams L.E., Retzlaff W.A., Yang W. *et al.*: Effect of girdling on leaf gas exchange, water status, and non-structural carbohydrates of field-grown *Vitis vinifera* L.(cv. Flame Seedless). – Am. J. Enol. Viticult. **51**: 49-54, 2000.

Yang J., Zhang J., Wang Z. *et al.*: Abscisic acid and cytokinins in the root exudates and leaves and their relationship to senescence and remobilization of carbon reserves in rice subjected to water stress during grain filling. – Planta **215**: 645-652, 2002.

Yang J., Zhang J., Wang Z. *et al.*: Involvement of abscisic acid and cytokinins in the senescence and remobilization of carbon reserves in wheat subjected to water stress during grain filling. – Plant Cell Environ. **26**: 1621-1631, 2003.

Yang X.Y., Wang F.F., Teixeira da Silva J.A. *et al.* Branch girdling at fruit green mature stage affects fruit ascorbic acid contents and expression of genes involved in l-galactose pathway in citrus. – N. Zeal. J. Crop Hort. **41**: 23-31, 2013.

Yordanov I., Goltsev V., Stefanov D. *et al.*: Preservation of photosynthetic electron transport from senescence-induced inactivation in primary leaves after decapitation and defoliation of bean plants. – J. Plant Physiol. **165**: 1954-1963, 2008.

Zwack P.J., Robinson B.R., Risley M.G. *et al.*: Cytokinin response factor 6 negatively regulates leaf senescence and is induced in response to cytokinin and numerous abiotic stresses. – Plant Cell Physiol. **54**: 971-981, 2013.